

Caesium-templated lanthanoid-containing polyoxotungstates

Firasat Hussain, Bernhard Spingler, Franziska Conrad, Manfred Speldrich,
Paul Kögerler, Colette Boskovic and Greta Ricarda Patzke*

Supporting Information

Synthesis S1: Synthesis, FT-IR and elemental analysis of compounds **Gd-1 – Er-1.** 2

Figure S2: Thermogravimetric data for **Eu-1 – Er-1.** 3

Figure S3: FT-IR spectra of compounds **Eu-1 – Er-1** (recorded in KBr, only the polyoxometalate “fingerprint region” is displayed). 4

Magnetic Measurements 5

Figure S4: Magnetization of **Gd-1** as a function of external field at 2.0 K. 6

Figure S5: Temperature dependence of the reciprocal susceptibility of **Gd-1.** 7

Synthetic Details S1:Synthesis, FT-IR and elemental analysis of compounds Gd-1 – Er-1.

Synthesis of polyanion **Gd-1**: A sample of Na₉[B- α -AsW₉O₃₃] (0.493 g, 0.20 mmol) was added with stirring to a solution of Gd(NO₃)₃·6H₂O (0.271 g, 0.60 mmol) in NaOAc/AcOH buffer (1.0 M, 25 mL) at pH 4.7. This solution was heated to 80 °C for 60 minutes and then cooled to room temperature and was filtered off to remove small amounts of precipitate. 2 ml of 0.5 M CsCl solution was added to the filtrate and the solution was stirred for 5 minutes and the resulting solution was left to evaporate. Yield (18%), FTIR of **Gd-1**: 951 (s), 859 (s), 785 (s), 707 (s), 635 (sh), 478 (m) cm⁻¹. Elemental analysis (%); calcd. (found): Na 2.5 (2.8), Cs 3.4 (3.3), As 2.3 (2.3), W 60.0 (58.8), Gd 4.9 (4.6).

Synthesis of polyanion **Tb-1**: Experimental procedure cf. above, Tb(NO₃)₃·6H₂O (0.261 g, 0.60 mmol) was used instead of Gd(NO₃)₃·6H₂O. Yield (15%), FTIR of **Tb-1**: 948 (s), 860 (s), 789 (s), 709 (s), 636 (sh), 480 (m) cm⁻¹. Elemental analysis (%); calcd (found): Na 2.5 (2.8), Cs 3.4 (3.4), As 2.3 (2.3), W 59.9 (58.6), Tb 4.9 (5.0).

Synthesis of polyanion **Dy-1**: Experimental procedure cf. above, Dy(NO₃)₃·6H₂O (0.263 g, 0.60 mmol) was used instead of Gd(NO₃)₃·6H₂O. Yield (13%), FTIR of **Dy-1**: 948 (s), 860 (s), 789 (s), 714 (s), 637 (sh), 481 (m) cm⁻¹. Elemental analysis (%); calcd. (found): Na 2.7 (2.8), Cs 4.3 (5.0), As 2.4 (2.1), W 62.8 (63.4), Dy 5.3 (5.2).

Synthesis of polyanion **Ho-1**: Experimental procedure cf. above, Ho(NO₃)₃·6H₂O (0.265 g, 0.60 mmol) was used instead of Gd(NO₃)₃·6H₂O. Yield (20%), FTIR of **Ho-1**: 948 (s), 861 (s), 789 (s), 713 (s), 636 (sh), 478 (m) cm⁻¹. Elemental analysis (%); calcd (found): Na 2.7 (2.7), Cs 4.3 (5.2), As 2.4 (2.1), W 62.8 (65.5), Ho 5.3 (5.2).

Synthesis of polyanion **Er-1**: Experimental procedure cf. above, Er(NO₃)₃·5H₂O (0.266 g, 0.60 mmol) was used instead of Gd(NO₃)₃·6H₂O. Yield (20%), FTIR of **Er-1**: 949 (s), 861 (s), 787 (s), 710 (s), 634 (sh), 477 (m) cm⁻¹. Elemental analysis (%); calcd. (found) : Na 2.7 (3.8), Cs 4.3 (5.0), As 2.4 (2.0), W 62.7 (59.5), Er 5.4 (5.4).

Elemental analyses of **Eu-1**, **Gd-1** and **Tb-1** were performed by Mikroanalytisches Labor Pascher, Remagen Germany and for **Dy-1**, **Ho-1** and **Er-1** by Zentrale Chemische Analytik (ZCH), Forschungszentrum Jülich, Jülich, Germany.

Supporting Information

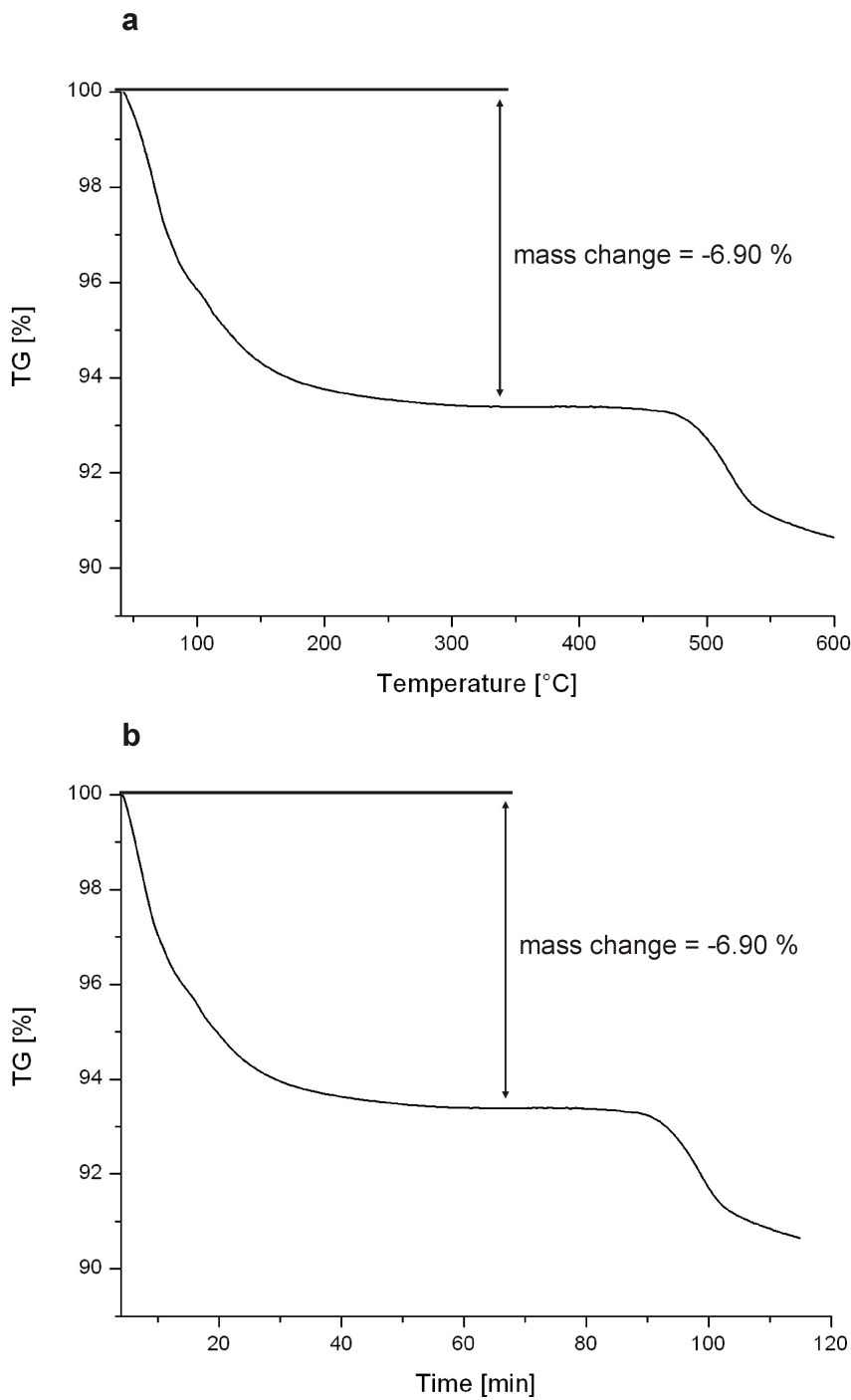


Figure S2. Representative thermogravimetric analysis of **Ho-1** displaying the mass loss corresponding to crystal water molecules (**Eu-1** = 7.22 %; **Gd-1** = 10.63 %; **Tb-1** = 5.78 %; **Dy-1** = 6.98 %; **Er-1** = 6.26 %).

TG measurements were performed on a Netzsch STA 449 C apparatus between 25 and 600 °C with a heating rate of 5 K/min in nitrogen atmosphere.

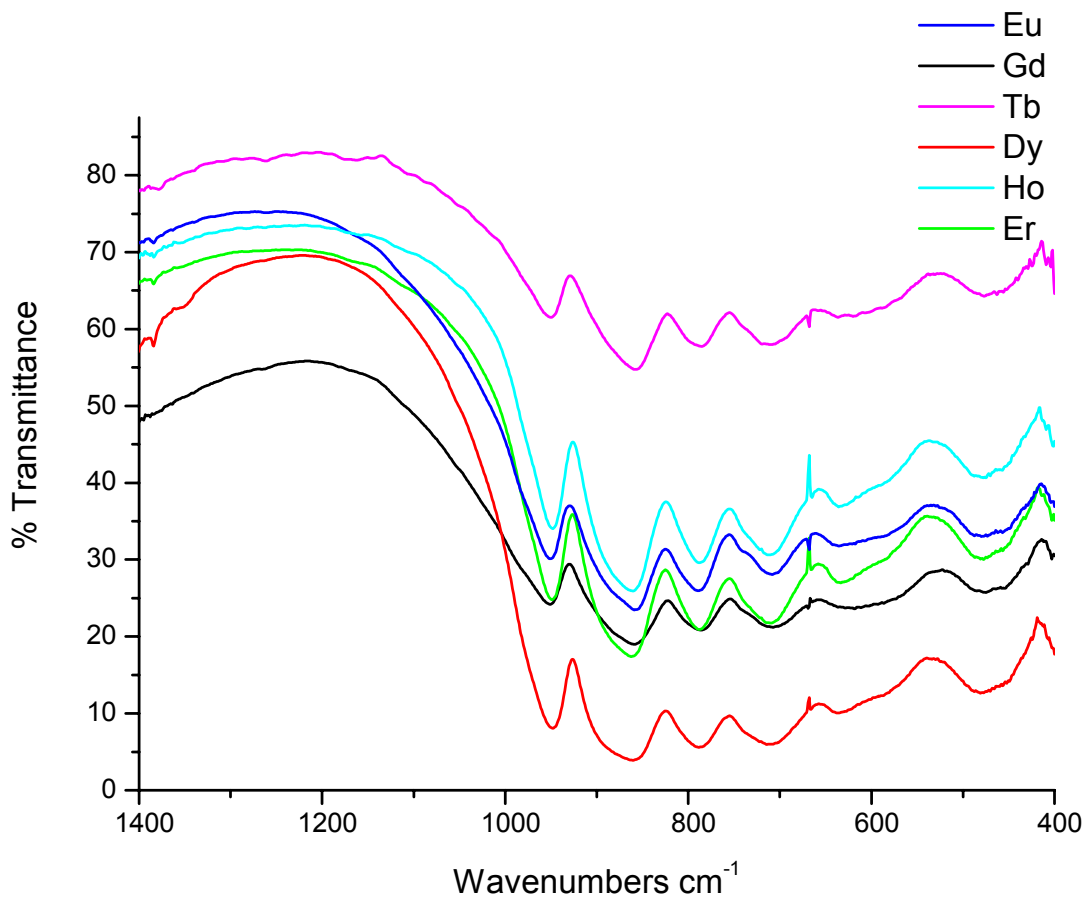


Figure S3. FT-IR spectra of compounds **Eu-1** – **Er-1** (recorded in KBr, only the polyoxometalate “fingerprint region” is displayed).

Magnetic Measurements

Magnetic susceptibility measurements were performed in a temperature range of 2 – 290 K for (**Gd-1**) at 0.1 – 5.0 T and for (**Er-1**) at 0.1 Tesla using a Quantum Design MPMS-5XL SQUID magnetometer. The experimental susceptibility values were corrected for the sample holder (Teflon tubes, the diamagnetic and temperature-independent paramagnetic (TIP) contributions of Gd³⁺ / Er³⁺ and the polyoxotungstate ligands ($\chi_{\text{dia/TIP}}(\text{Gd-1}) = -35.0 \times 10^{-9} \text{ m}^3 \text{ mol}^{-1}$; $\chi_{\text{dia/TIP}}(\text{Er-1}) = -32.0 \times 10^{-9} \text{ m}^3 \text{ mol}^{-1}$).^[1, 2]

Theoretical modeling: We consider a magnetically isolated f^N metal ion surrounded by ligands imposing a distinct point symmetry upon the magnetic center. In a static magnetic field **B** the Hamiltonian of the metal ion is then represented by

$$\hat{H} = \underbrace{\sum_{i=1}^N \left[-\frac{\hbar^2}{2m_e} \nabla_i^2 + V(r_i) \right]}_{\hat{H}^{(0)}} + \underbrace{\sum_{i>j}^N \frac{e^2}{r_{ij}}}_{\hat{H}_{ee}} + \underbrace{\sum_{i=1}^N \zeta(r_i) \kappa \hat{l}_i \cdot \hat{s}_i}_{\hat{H}_{so}} + \underbrace{\sum_{i=1}^N \sum_{k=0}^{\infty} \left\{ B_0^k C_0^k(i) + \sum_{q=2}^k \left[B_q^k \left(C_{-q}^k(i) + (-1)^q C_q^k(i) \right) \right] \right\}}_{\hat{H}_{LF}} + \underbrace{\sum_{i=1}^N \mu_B (\kappa \hat{l}_i + 2 \hat{s}_i) \cdot \mathbf{B}}_{\hat{H}_{mag}} \quad (1)$$

While $H^{(0)}$ represents the energy in the central field approximation, H_{ee} and H_{so} account for interelectronic repulsion and spin-orbit coupling (modified by the orbital reduction factor κ), respectively. The former is taken into account by the Slater-Condon parameters F², F⁴, F⁶, the latter by the one-electron spin-orbit coupling parameter ζ . These sets of interelectronic repulsion parameters as well as ζ and κ are used as constants in the fitting calculations.

H_{LF} gives the electrostatic effect of the ligands in the framework of ligand field theory on the basis of the global parameters B_q^k . The spherical tensors C_q^k are directly related to the spherical harmonics

$C_q^k = \sqrt{4\pi/(2k+1)} Y_q^k$ and the real ligand field parameters B_q^k (Wybourne notation^[3, 4]) are given by

$A_q^k \langle r^k \rangle$ where A_q^k is a numerical constant describing the charge distribution in the environment of the metal ion and $\langle r^k \rangle$ is the expectation value of $\langle r^k \rangle$ for the wave function.

For f electrons the terms in the expansion with $k \leq 6$ are nonzero, whereas all terms with odd k values vanish since we consider only configurations containing equivalent electrons. The values of k and q are limited by the point symmetry of the metal ion site.

Supporting Information

If the spherically symmetric term $B_0^0 C_0^0$ (which does not cause any splitting) is ignored, in cubic systems only spherical tensors with $k = 4$ and $k = 6$ are relevant and all B_q^k are zero. The ligand field operator with reference to the fourfold rotation axis for the angular part of the wave function reads.

$$H_{LF}^{tet} = B_0^2 \sum_{i=1}^N C_0^2(i) + B_0^4 \sum_{i=1}^N [C_0^4(i) + \sqrt{5/14}(C_4^4(i) + C_{-4}^4(i))] + B_0^6 \sum_{i=1}^N [C_0^6(i) - \sqrt{7/2}(C_4^6(i) + C_{-4}^6(i))]$$

For magnetochemical analyses, we developed the computer program CONDON.^[5] For modeling the magnetic behaviour of the 4f-system (**Gd-1**) interelectronic repulsion (H_{ee}) and spin-orbit-coupling (H_{so}) and (**Er-1**) interelectronic repulsion (H_{ee}), spin-orbit-coupling (H_{so}) and lf effect (H_{LF}), has to be taken into account.

In order to determine the magnetic behaviour of (**Gd-1**) we use only the Slater Condon Parameter ($^2F = 91\ 800\ \text{cm}^{-1}$, $^4F = 64\ 425\ \text{cm}^{-1}$, $^6F = 49\ 258\ \text{cm}^{-1}$), the spin orbit-coupling constant ($\zeta = 1\ 470\ \text{cm}^{-1}$) and the applied magnetic field ($B_0 = 0.1, 0.5, 1, 2, 3, 4, 5\ \text{T}$).^[6, 7] The magnetochemical analyses show a g-value of 1.993 with the corresponding magnetic moment of 7.91. The reduce g-value is a result of the large spin-orbit interaction that mixes significant amounts of other terms into with $J = 7/2$ into the ground state. The major SL components of the ground state are 8S (97 %) and 6P (2.7 %) with the corresponding g_J factor 1.993.^[8]

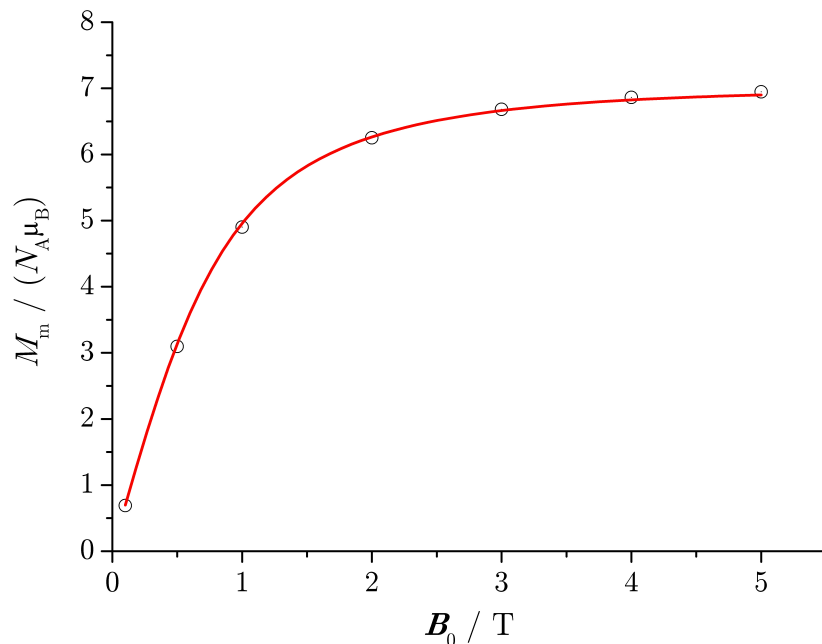


Figure S4. Magnetization as a function of external field at 2.0 K, showing a Brillouin-type behavior (experimental data: open circles, best fit: red graph). Parameters employed: $S = 7/2$, $g_J = 1.993$ and $\text{SQ} = 0.18\ \%$.

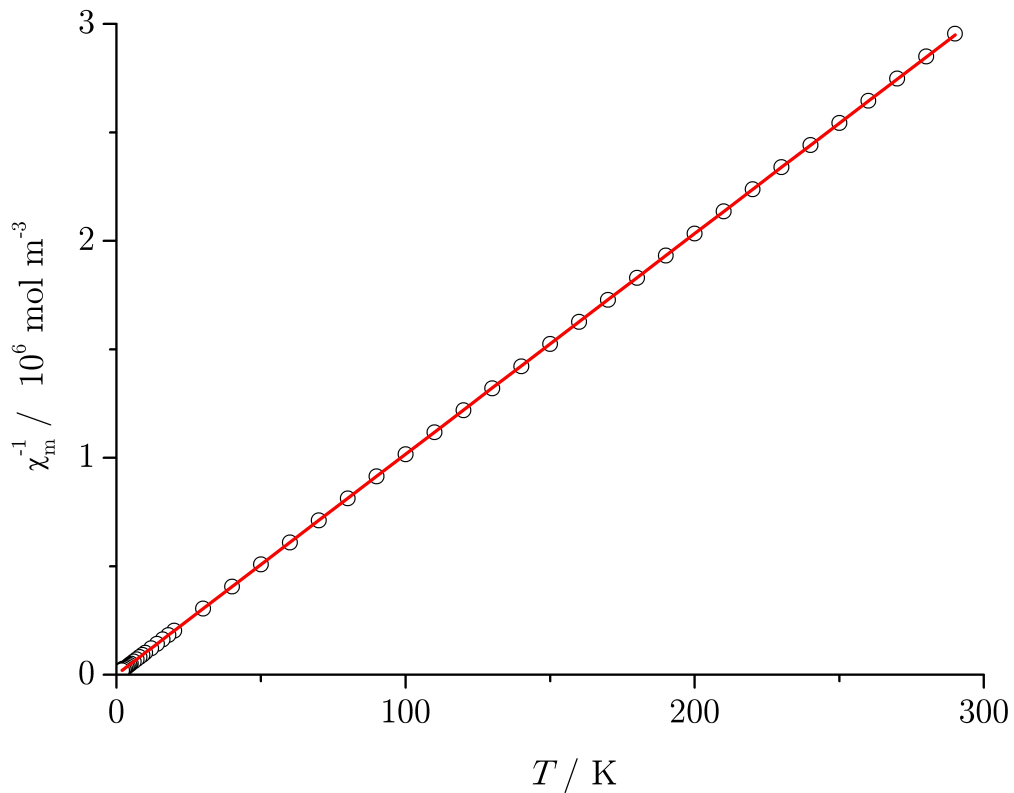


Figure S5. Temperature dependence of the reciprocal susceptibility (χ_m^{-1}) of (Gd-1) at 0.1 Tesla emphasizing the near perfect Curie paramagnetism (experimental data: open circles, best fit: red graph); see text for parameters.

In the case of Er (III), the consideration of the ligand field effect (H_{lf}) is especially important. To reduce the number of lf parameters, the local point symmetry C_s ; (15 independent lf parameters) was idealised to D_{4h} (3 independent lf parameters). The initial set of B_q^k parameter values was taken from spectroscopically determined energy levels for Er(III) in cubic elpasolite crystals.^[10]

In order to determine the corresponding ligand field parameters B_q^k the assumption of D_{4h} symmetry was sufficient to yield an excellent fit (Figure 3; SQ 0.4%) $B_0^2 = 240 \text{ cm}^{-1}$, $B_0^4 = 1550 \text{ cm}^{-1}$, $B_0^6 = 230 \text{ cm}^{-1}$ and a spin-orbit coupling parameter $\zeta = 2369 \text{ cm}^{-1}$.

Supporting Information

The following fitting procedure was employed:

- (1) Starting parameters for a cubic Er (III) system (B_0^4 and B_0^6); the corresponding compound is listed in ref. 10.
- (2) The ratios between the parameters B_0^4 and B_4^4 as well as B_0^4 and B_4^4 were set as constant, reflecting cubic ligand field symmetry ($B_4^4 = \sqrt{5/14} B_0^4$ and $B_4^6 = \sqrt{7/2} B_0^6$).^[10] Note that the quality of the fit does not increase significantly upon removing these constraints.
- (3) To accommodate the assumed near-tetragonal symmetry of the Er (III) ligand field, a third free parameter B_0^2 was introduced.
- (4) The (fixed) spin-orbit coupling parameter was chosen as $\zeta = 2369 \text{ cm}^{-1}$ according to ref. 10.

References

- [1] W. Haberditzl, *Angew. Chem.* 1966, **78**, 277 – 288.
- [2] H. Lueken, *Magnetochemie*, Teubner, Stuttgart 1999, pp. 426 – 427.
- [3] B.G. Wybourne, *Spectroscopic Properties of Rare Earths*, Wiley, New York, London, Sydney 1965.
- [4] C. Görller-Walrand, K. Binnemans, Rationalization of crystal-field parametrization, in: K.A. Gschneidner, Jr., L. Eyring (Eds.), *Handbook on the Physics and Chemistry of Rare Earths*, Vol. 23, Ch. 155, p. 121, Elsevier, Amsterdam, 1996.
- [5] H. Schilder and H. Lueken, *J. Magn. Magn. Mat.* 2004, **281**, 17 – 26.
- [6] E. U. Condon and G. H. Shortley, *The Theory of Atomic Spectra*, Cambridge University Press, Cambridge, 1953.
- [7] S. Hüfner, *Optical Spectra of Transparent Rare Earth Compounds*, Academic Press, Inc. New York, 1978.
- [8] J. Sytsma, K. M. Murdoch, N. M. Edelstein, L. A. Boatner and M. M. Abraham, *Phys. Rev. B* 1995, **52**, 12668 – 12676
- [9] A. J. Shuskus, *Phys. Rev.* 1962, **127**, 2022 – 2024.
- [10] P. A. Tanner, V. V. Ravi Kanth Kumar, C. K. Jayasankar, M. F. Reid, Analysis of spectral data and comparative energy level parametrizations for Ln^{3+} in cubic elpasolite crystals, *J. Alloys Comp.* 1994, **215**, 349 – 370.